Received: 29 September 2023 | Revised: 19 December 2023 | Accepted: 23 December 2023

DOI: 10.1002/jcc.27305

RESEARCH ARTICLE

Journal of COMPUTATIONAL CHEMISTRY WILEY

# Theoretical prediction of closed-shell paramagnetism for scandium and yttrium hydride

Laura Grazioli[1] | Luca T. Schleicher[1] | Stella Stopkowicz[2,3] | Jürgen Gauss[1]

[1]Department Chemie, Johannes Gutenberg-Universität Mainz, Mainz, Germany

[2]Fachrichtung Chemie, Universität des Saarlandes, Saarbrücken, Germany

[3]Hylleraas Centre for Quantum Molecular Sciences, Department of Chemistry, University of Oslo, Oslo, Norway

**Correspondence**
Jürgen Gauss, Department Chemie, Johannes Gutenberg-Universität Mainz, Duesbergweg 10-14, D-55128, Mainz, Germany.
Email: gauss@uni-mainz.de

## Abstract

Following chemical intuition, one would expect that all closed-shell molecules are diamagnetic. However, it is known that this is not the case for some second-row hydrides with low-lying unoccupied $\pi$ orbitals due to an unquenching of the total angular momentum in the presence of an external magnetic field. In this article, the transition-metal hydrides ScH and YH are investigated, assuming a similar unquenching effect involving low-lying unoccupied $\pi$ and $\delta$ orbitals formed from the metal *d* orbitals rather than the *p* orbitals. We are comparing results obtained with various quantum-chemical methods (HF, CCSD, CCSD(T), CCSDT) and basis sets. The obtained positive values for the magnetizabilities clearly indicate paramagnetic behavior. Vibrational effects on the magnetizability tensor are also considered, but these effects are small and do not change the overall conclusion that both ScH and YH are further examples for closed-shell paramagnetism.

**KEYWORDS**
closed-shell paramagnetism, coupled-cluster calculations

## 1 | INTRODUCTION

Contrary to common chemical and physical intuition, not all closed-shell molecules are diamagnetic. It has been predicted quite some time ago that there exist closed-shell species with a temperature-independent (so-called *Van Vleck*) paramagnetism,[1–3] for example, BH and related hydrides of the second and third period[4–6] as well as $MnO_4^-$.[7] Earlier proofs of compulsory diamagnetism for closed-shell molecules have been shown later to be wrong and hold only for less than three electrons.[8] Thus, paramagnetic behavior is indeed theoretically possible for closed-shell molecules with more electrons. This surprising computational finding can be explained by the partial unquenching of the angular momentum in the presence of an external magnetic field.[9]

In Reference 4, hydrides of the second and third period (BH, $CH^+$, $BeH^-$, AlH, $GeH^+$, $MgH^-$) have been investigated using quantum-chemical calculations and actually for some of them (BH, $CH^+$) paramagnetic behavior has been unequivocally predicted. With a lack of experimental data for BH and $CH^+$, a first, though indirect experimental evidence for the possible paramagnetism of BH comes from the experimental estimate for the rotational *g* factor of AlH, where the perpendicular component of the total magnetizability has been shown to be paramagnetic.[10] For the hydrides of the second and third period, the unquenching of the angular momentum is due to unoccupied $\pi$ orbitals that also account for low-lying $\Pi$ excited states. However, the important role of the diamagnetic contribution (due to number of electrons and occupied orbitals) has also been stressed and the conclusion was that paramagnetism in these hydrides decreases from the left to the right as well as from the top to the bottom in the periodic table. Noting the necessity of unoccupied and low-lying $\pi$ orbitals for closed-shell paramagnetism in diatomic species, it is an obvious question whether paramagnetism can be found for the analogous transition-metal hydrides, with $\pi$ and $\delta$ orbitals arising from *d* orbitals (instead of *p* orbitals).

In this work, we will answer this question and investigate the hydrides of scandium and yttrium, that is, ScH and YH, by means of high-level quantum-chemical calculations. These two hydrides appear most promising considering their similarity to BH, with the only difference that the low-lying unoccupied $\pi$ (and $\delta$) orbitals are formed from *d* orbitals.

We start by discussing the underlying theory of closed-shell paramagnetism together with some remarks on the quantum-chemical calculation of the magnetizability and the closely related rotational *g* tensor. This is followed by a section describing the computational details of our quantum-chemical investigation. We discuss our results in particular with respect to our initial question concerning the possible closed-shell paramagnetism of ScH and YH and then finish with some concluding remarks.

## 2 | THEORY

When a molecule is exposed to a magnetic field **H**, the energy varies with the strength of the magnetic induction **B**. To investigate this dependence theoretically, the energy may be expanded in a Taylor series around its zero-field value

$$E(\mathbf{B}) = (E)_{B=0} + \left(\frac{\partial E}{\partial \mathbf{B}}\right)^{\top}_{B=0} \cdot \mathbf{B} + \frac{1}{2}\mathbf{B}^{\top} \cdot \left(\frac{\partial^2 E}{\partial \mathbf{B} \partial \mathbf{B}}\right)_{B=0} \cdot \mathbf{B} + \cdots \quad (1)$$

The first derivatives of the energy with respect to the components of the magnetic-induction vector represent the components of the permanent magnetic-moment vector $\mathbf{m} = -\left(\frac{\partial E}{\partial \mathbf{B}}\right)_{B=0}$, while the second derivatives (apart from the sign) define the magnetizability tensor $\boldsymbol{\xi} = -\left(\frac{\partial^2 E}{\partial \mathbf{B} \partial \mathbf{B}}\right)_{B=0}$. From the perspective of electromagnetism, the permanent magnetic moment of a particle with charge *q* and mass *m* is given by

$$\mathbf{m} = \frac{q}{2m}\mathbf{J}, \quad (2)$$

where **J** is the total angular momentum, obtained as the sum of the rotational angular momentum **L** and the spin **S**: $\mathbf{J} = \mathbf{L} + \mathbf{S}$. In the case of closed-shell molecules, the total angular momentum is completely quenched and there are no unpaired spins, resulting necessarily in a vanishing permanent magnetic moment.

The presence of an external field, however, gives rise to an induced magnetic moment, which is linked to the magnetizability

$$\mathbf{m}_{\text{ind}} = \xi \mathbf{B}. \quad (3)$$

Usually, the magnetic behavior of a given system is described macroscopically through the susceptibility $\chi$, which, multiplied by the magnetic field **H**, defines the macroscopic magnetization **M**

$$\mathbf{M} = \chi \mathbf{H}. \quad (4)$$

When $\chi < 0$, the sample is diamagnetic; otherwise, if $\chi > 0$, it is paramagnetic. For closed-shell molecules, which do not possess a permanent magnetic moment, the magnetizability alone contributes to the susceptibility. The connection from the microscopic to the macroscopic description is given by $\chi \approx N\mu_0\xi$, where *N* is the number density of the sample and $\mu_0$ the magnetic permeability of the vacuum. The relation between the sign and the magnetic behavior can therefore be transferred to $\xi$. In this work, the sign of the isotropic magnetizability, defined as the trace of the corresponding tensor, will be used as the indicator for paramagnetic behavior: for $\text{Tr}\{\xi\} < 0$, the molecule is diamagnetic, for $\text{Tr}\{\xi\} > 0$, paramagnetic.

The possibility of paramagnetism in closed-shell systems has been a quite lengthy topic in quantum chemistry. Van Vleck[1–3] developed an elaborate formalism, in which the susceptibility is split into a diamagnetic and a paramagnetic part: $\chi = \chi_{\text{dia}} + \chi_{\text{para}}$. Guy et al.[11,12] postulated that $|\chi_{\text{dia}}| > |\chi_{\text{para}}|$ for closed-shell molecules, necessarily leading to diamagnetic behavior for these systems. Later, Rebane[8,13] showed that this proof is only valid in the case of a one-electron function without nodes; such a function, however, allows only the occupation with up to two electrons.

Following Reference 9, the Van Vleck definition of a diamagnetic and a paramagnetic part in the susceptibility may be used to analyze the magnetic behavior of closed-shell molecules. In particular, we can describe the process of the formation of a diatomic closed-shell species from the perspective of interacting momenta. The spins become oppositely paired and the total angular momentum results from the sum of the single angular momenta, as an effect of the interaction between the two atoms. The total angular momentum becomes quantized and the component perpendicular to the internuclear axis is quenched, in such a way that the expectation value of each component vanishes, while the angular momentum squared is still non-vanishing. This is due to fluctuations between the electronic angular momentum and the momentum arising from the molecular motion.[9]

When exposing a molecule to a magnetic field, the net angular momentum tends to be aligned to it, causing a partial unquenching, resulting in a non-zero average value of the angular-momentum component aligned to the field itself. This effect contributes to the paramagnetic susceptibility, while the opposed Larmor precession contributes to the diamagnetic part. Which effect dominates determines the final magnetic character of the system. Thus a large quenched angular momentum in the field-free setting will most likely enable a large amount of unquenching when turning on the magnetic field. This may favor a paramagnetic behavior in a closed-shell system.

Van Vleck used second-order perturbation theory to derive a mathematical expression for the magnetizability[3]:

$$\xi(\mathbf{R}_O) = \xi_{\text{dia}}(\mathbf{R}_O) + \xi_{\text{para}}(\mathbf{R}_O) = -\frac{e^2}{4m_e}\sum_i^{N_{\text{el}}} \langle 0|(\mathbf{r}_i - \mathbf{R}_O)\cdot(\mathbf{r}_i - \mathbf{R}_O) - (\mathbf{r}_i - \mathbf{R}_O)(\mathbf{r}_i - \mathbf{R}_O)|0\rangle - \frac{e^2}{2m_e^2}\sum_n \frac{\langle 0|\left(\sum_i (\mathbf{r}_i - \mathbf{R}_O)\times \mathbf{p}_i\right)|n\rangle\langle n|\left(\sum_j (\mathbf{r}_j - \mathbf{R}_O)\times \mathbf{p}_j\right)|0\rangle}{E_0 - E_n}, \quad (5)$$

where the first term is the diamagnetic part and the second the paramagnetic one. The index $i$ labels the electrons, while $n$ runs over the set of excited states. Both terms depend on the position $\mathbf{R}_O$ (gauge origin) used to define the gauge. This dependence is a common feature of magnetic properties due to the presence of the angular-momentum operator in the magnetic-field Hamiltonian (see Section 2.1). In general, there is no unique choice for the gauge origin, making results dependent on the choice of $\mathbf{R}_O$. On the other hand, physical observables must be independent of this choice (gauge-origin invariance), a feature which should also be maintained in the quantum-chemical description. It can be shown[3] that both terms in Equation (5) depend on the gauge origin $\mathbf{R}_O$ and thus cannot be observables on their own; only their sum is a physical observable and is gauge-origin independent.

The diamagnetic part is found to be always negative, while the paramagnetic part is positive for closed-shell molecules and, usually, much smaller in magnitude. Therefore, in order to have closed-shell paramagnetism, the condition $|\xi_{\text{para}}| > |\xi_{\text{dia}}|$ must hold.

## 2.1 | Quantum-chemical calculation of magnetizabilities

The magnetizability tensor $\boldsymbol{\xi}$ is defined via the second derivatives of the electronic energy with respect to the components of an external magnetic induction $\mathbf{B}$ (with a negative sign)

$$\xi_{rs} = -\left(\frac{\partial^2 E}{\partial B_r \partial B_s}\right)_{B=0}. \tag{6}$$

The Hamiltonian of a molecular system in a magnetic field can be written as a sum of the unperturbed Hamiltonian operator $\hat{H}_0$ and the following additional terms

$$H = H_0 + \frac{1}{2}\mathbf{B}\cdot\mathbf{L}(\mathbf{R}_O) + \mathbf{B}\cdot\mathbf{S} + \frac{1}{8}\sum_i^N (B^2 r_{iO}^2 - (\mathbf{B}\cdot\mathbf{r}_{iO})^2) \tag{7}$$

with

$$\mathbf{r}_{iO} = \mathbf{r}_i - \mathbf{R}_O. \tag{8}$$

The terms coupling the magnetic field to the angular momentum $\mathbf{L}(\mathbf{R}_O)$ (*orbital-Zeeman* term) and to the spin operator $\mathbf{S}$ (*spin-Zeeman* term) are usually referred to as *paramagnetic terms*. They tend to stabilize states with either high angular momentum or spin. The form of the angular momentum evidences the dependence of these terms on the gauge origin $\mathbf{R}_O$

$$\mathbf{L}(\mathbf{R}_O) = \sum_i (\mathbf{r}_i - \mathbf{R}_O) \times \mathbf{p}_i \tag{9}$$

with the sum over index $i$ running over the electrons of the molecular system. The terms quadratic in the magnetic induction in Equation (7) are called *diamagnetic terms*. These are always positive and act as confining potential in the plane perpendicular to the magnetic field.

A way to ensure gauge-origin independent results in a quantum-chemical calculation is to use gauge-including atomic orbitals (GIAOs, also known as London orbitals)[14–17]:

$$\omega_\mu(\mathbf{B}) = \exp(-i\mathbf{A}_\mu^\mathbf{B}\cdot\mathbf{r})\chi_\mu \tag{10}$$

with $\chi_\mu$ as the corresponding field-free basis function centered at $\mathbf{R}_\mu$ and $\mathbf{A}_\mu^\mathbf{B}$ as the vector potential at the center $\mathbf{R}_\mu$ of the function $\chi_\mu$:

$$\mathbf{A}_\mu^\mathbf{B} = \frac{1}{2}\mathbf{B}\times(\mathbf{R}_\mu - \mathbf{R}_O). \tag{11}$$

The use of GIAOs guarantees gauge-origin independence of the results and also speeds up their basis-set convergence.[17] Computationally, however, the dependence of the basis functions on the magnetic induction $\mathbf{B}$ leads to the necessity to compute additional one- and two-electron integrals.[16–18]

The calculation of the magnetizability tensor using GIAOs has been first reported by Ruud et al. at the Hartree-Fock (HF) level.[19] The electron-correlated calculation of magnetizabilities (at second-order Møller-Plesset perturbation theory (MP2)[20] and at many coupled-cluster (CC) levels including the CC singles and doubles (CCSD),[21] CC singles, doubles, and perturbative triples (CCSD(T)[22]), and CC singles, doubles, and triples (CCSDT)[23,24] schemes) has been described somewhat later by Gauss et al.[25] Details of the corresponding implementations can be found in the original references.

## 2.2 | Vibrational corrections

For comparison with experiment, it is usually important to augment the computational results with zero-point vibrational effects. For this purpose, the magnetizability tensor can be expanded in a Taylor series up to second order around the equilibrium geometry with respect to the normal coordinates $Q_r, Q_s, \ldots$ of the molecule. Averaging over the vibrational ground state then yields the vibrationally averaged magnetizability[26,27]

$$\begin{aligned}\langle\xi\rangle \approx\ & \xi_0 + \sum_r \left(\frac{\partial\xi}{\partial Q_r}\right)_{Q_r=0}\langle Q_r\rangle \\ & + \frac{1}{2}\sum_{rs}\left(\frac{\partial^2\xi}{\partial Q_r \partial Q_s}\right)_{Q_r,Q_s=0}\langle Q_r Q_s\rangle,\end{aligned} \tag{12}$$

where the expressions for the expectation values of the normal-mode displacements are given by References 27 and 28

$$\langle Q_r\rangle = \sqrt{\frac{1}{2\hbar\omega_r^3}}\sum_s \phi_{rss}, \tag{13}$$

$$\langle Q_r Q_s\rangle = \delta_{rs}\frac{\hbar}{4\omega_r}. \tag{14}$$

Here $\omega_r$ is the harmonic frequency of the $r$th normal mode and $\phi_{rst}$ is the corresponding cubic force constant in normal-coordinate

representation, most conveniently computed by numerical differentiation of analytically calculated harmonic force fields[25] with respect to $Q_r$.[29,30] Note that both the harmonic and the anharmonic terms are needed to obtain vibrational corrections up to second order.

### 2.3 | Rotational *g* tensor

To verify closed-shell paramagnetism experimentally, gas-phase measurements of a quantity closely related to the magnetizability tensor, the rotational *g* tensor, can be carried out.[31] It is therefore of interest to calculate this quantity directly. In the presence of an external magnetic field the rotational-energy levels of a molecular system depend on the magnetic induction due the interaction of the induced magnetic moment of the molecule with the external field. This dependence is described through the rotational *g* tensor, which is related to the paramagnetic term in the magnetizability.[31] The rotational *g* tensor can be expressed as an energy derivative with respect to **B** and **J** via

$$\mathbf{g} = -\frac{\hbar}{\mu_N}\left(\frac{\partial^2 E}{\partial \mathbf{B}\partial \mathbf{J}}\right)_{B,J=0}, \tag{15}$$

where $\mu_N$ denotes the nuclear magneton. Though there is a preferred choice for the gauge origin of the vector potential in the case of the rotational *g* tensor, in order for results to be rigorously (gauge-)origin independent in quantum-chemical calculations and to speed up the basis-set convergence in the calculations, it is the best to use GIAOs in the actual computations tensor. In that case the so-called rotational London orbitals must be used[32]

$$\omega_\mu(\mathbf{B},\mathbf{J}) = \exp\left[-i\left(\mathbf{A}_\mu^{\mathbf{B}} + \mathbf{A}_\mu^{\mathbf{J}}\right)\cdot\mathbf{r}\right]\chi_\mu, \tag{16}$$

where $\mathbf{A}_\mu^{\mathbf{B}}$ denotes the vector potential associated with the external magnetic field and $\mathbf{A}_\mu^{\mathbf{J}}$ the vector potential of the field induced by the rotational motion.

Following Reference 32, the link between the rotational *g* tensor and the magnetizability tensor computed using GIAOs is

$$\mathbf{g} = -4M_P\left(\xi^{\mathrm{GIAO}} - \xi^{\mathrm{dia}}(\mathrm{c.m.})\right)\mathbf{I}^{-1} + \mathbf{g}^{\mathrm{nuc}}, \tag{17}$$

where $M_P$ is the proton mass, **I** is the inertia tensor of the molecule and $\mathbf{g}^{\mathrm{nuc}}$ represents the nuclear contribution to **g**. The superscript GIAO indicates that the magnetizability tensor is computed using GIAOs, while the diamagnetic contribution $\xi^{\mathrm{dia}}(\mathrm{c.m.})$ is computed with the center of mass (c.m.) as gauge origin and without GIAOs. The paramagnetic part of the magnetizability tensor is here linked as follows to the magnetizability tensor, computed with GIAOs, and the corresponding diamagnetic contribution, computed at the center of mass[32]

$$\xi^{\mathrm{para}} = \xi^{\mathrm{GIAO}} - \xi^{\mathrm{dia}}(\mathrm{c.m.}). \tag{18}$$

The rotational *g* tensor is an interesting quantity to be analyzed when inspecting the magnetic behavior of a molecule. Large negative values can be taken as an indication for paramagnetism. Therefore, we report in the following also our results for the rotational *g* tensor including corresponding zero-point vibrational corrections.

## 3 | COMPUTATIONAL DETAILS

Calculations were carried out at different levels of theory, starting with HF, followed by CCSD,[21] CCSD(T),[22] and CCSDT.[23,24] In the case of ScH, two basis-set families are used, that is, cc-pVXZ with X=T, Q, 5, and cc-pwCVXZ with X=T, Q, 5).[33,34] In the case of the cc-pVXZ basis sets, the frozen-core (fc) approximation has been used, while with the cc-pwCVXZ basis sets all electrons were considered in the electron-correlation treatment. For YH, the ANO-RCC basis set[35,36] was used in its uncontracted form and all electrons were correlated. Geometry optimizations were performed using analytic gradients at the corresponding levels of theory.[37–39] HF results were converged using the quadratically convergent self-consistent field (QCSCF) scheme[40] to maximal changes in the density-matrix elements less than $\delta = 10^{-8}$; the various types of CC equations (i.e., unperturbed and perturbed amplitude and $\Lambda$ equations) were considered converged when the maximum of all absolute changes in the corresponding amplitudes was less than $\delta = 10^{-8}$. Geometry optimizations were considered converged when the root mean square gradient was less than $\delta = 10^{-4}$ Hartree/bohr.

Both ScH and YH are linear diatomic molecules with $C_{\infty v}$ symmetry. Computationally, the largest Abelian subgroup $C_{2v}$ of this non-Abelian point group is used. In order to converge to the correct ground state, the occupation has been fixed as follows (the order of the irreducible representations of $C_{2v}$ is denoted as $A_1/B_1/B_2/A_2$:

1. the 22 electrons of ScH are distributed, in the restricted HF ansatz, as 7/2/2/0 both for $\alpha$ and $\beta$;
2. the 40 electrons of YH are distributed, in the restricted HF ansatz, as 11/4/4/0 both for $\alpha$ and $\beta$.

We note already here that relativistic effects are not considered in the present study. Certainly, their inclusion is recommended for the highly accurate determination of the equilibrium geometry and magnetic properties of ScH and in particular of YH. Corresponding methods are in principle available,[41–43] but such calculations are not necessary for the purpose of the present investigation.

All calculations were performed with a development version of the CFOUR program package.[44,45]

## 4 | RESULTS

We start with a discussion of the computed equilibrium geometries. This is followed by an in-depth discussion of our results for the

magnetic properties of interest, that is, magnetizability and rotational *g* tensor, with a focus on electron correlation, basis-set convergence, and zero-point vibrational contributions.

## 4.1 | Equilibrium geometries

Geometry optimizations were performed for both ScH and YH. The results depend on both the used method to treat electron correlation and the used basis set. In Table 1, the obtained geometries and energies for ScH are shown for the different methods when using the cc-pV5Z and cc-pwCV5Z basis sets, respectively. Table 2 shows the corresponding results for YH when using the uncontracted ANO basis set. The trends in the computational results can be more easily seen in Figure 1, where the equilibrium bond length is shown for both hydrides as a function of the used quantum-chemical method. For ScH, the calculations with the cc-pV5Z and cc-pwCV5Z sets show a somewhat different behavior. While with the cc-pwCV5Z set the expected shortening of the bond distance due to inclusion of electron correlation is seen, this typical trend is not seen in the cc-pV5Z calculations. This difference as well as the magnitude of the correlation effects are most likely explained by the fact that all calculations with the cc-pV5Z set were carried out within the fc approximation, thus not considering core-valence correlation effects which are known to be important for the accurate prediction of equilibrium structures.[46] CCSD and CCSD(T) lead to longer bond distances, which with the cc-pwCV5Z set are still significantly shorter (by about 0.02 Å) than the corresponding HF bond distance. Effects due to a full treatment of triple excitations at the CCSDT level turn out to be negligible and amount to less than 0.0002 Å when using the cc-pV5Z basis set (the effect might be larger with the cc-pwCV5Z set, but corresponding CCSDT computations were too demanding with the available computational resources). To demonstrate the high accuracy of our computational results, we mention that our best value of 1.7574 Å, obtained at the CCSD(T)/cc-pwCV5Z level, compares well with the experimentally determined bond distance of 1.775427(8) Å[47] and to other computational results, ranging from 1.76216 Å to 1.8124 Å.[48–50]

**TABLE 1** Equilibrium bond length *R* (in Ångström) and corresponding energy *E* (in Hartree) of ScH computed with different methods using the cc-pV5Z and cc-pwCV5Z basis sets.

| cc-pV5Z | *E* | *R* |
|---|---|---|
| HF | −760.2779 | 1.7767 |
| CCSD | −760.3636 | 1.7908 |
| CCSD(T) | −760.3663 | 1.7925 |
| CCSDT | −760.3668 | 1.7927 |
| **cc-pwCV5Z** | ***E*** | ***R*** |
| HF | −760.2780 | 1.7766 |
| CCSD | −760.9349 | 1.7504 |
| CCSD(T) | −760.9550 | 1.7574 |

**TABLE 2** Equilibrium bond length *R* (in Ångström) and corresponding energy *E* (in Hartree) of YH computed with different methods using the uncontracted ANO-RCC basis set.

| Method | *E* | *R* |
|---|---|---|
| HF | −3332.2589 | 1.9387 |
| CCSD | −3333.6528 | 1.9078 |
| CCSD(T) | −3333.6764 | 1.9087 |

For YH, HF gives a longer distance than CC and our best value obtained at the CCSD(T)/uncontracted ANO-RCC level compares well with the experimental value of 1.922765(8) Å,[51] better than other computational results of about 1.865 Å.[52]

We also note that the most serious shortcoming of our computations is the neglect of relativistic effects.[53] They should definitely be included to reach quantitative agreement with experiment, but their consideration is less important for the purpose of the present computational investigation, in which we are aiming at a qualitative prediction of paramagnetism.

For ScH, the computed equilibrium bond lengths can be also analyzed with respect to its basis-set dependence (Table 3). Here all calculations were performed at the CCSD(T) level of theory. For the cc-pVXZ family, only slight variations are observed, while for the cc-pwCVXZ family the effects are more pronounced due to the additional consideration of core-valence correlation.

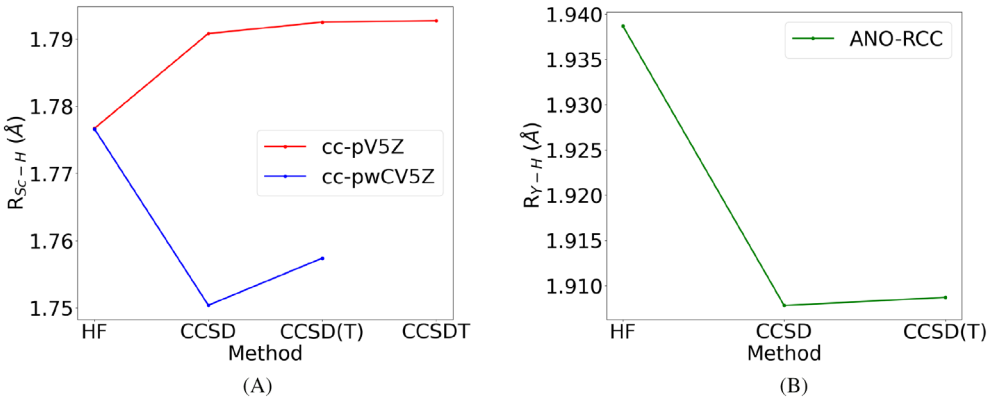


**FIGURE 1** Equilibrium geometries of ScH (left) and YH (right) in Ångström, calculated at HF, CCSD, CCSD(T), and CCSDT levels of theory. The red line corresponds to results for ScH obtained with the cc-pV5Z basis set, the blue one to results for ScH obtained with the cc-pwCV5Z and the green one to results for YH obtained with the uncontracted ANO-RCC basis set.

The equilibrium bond length shortens and remaining basis-set effects are estimated to be of the order of a few hundredths Ångström.

## 4.2 | Magnetic properties

This section deals with our results for the magnetizability and rotational $g$ tensors of ScH and YH (when listing the values of $\xi$, we are referring to the corresponding isotropic quantities, that is, one third of the trace of the corresponding tensor; for $g$ we are listing the $xx$ component of the diagonal tensor, as $g_{xx} = g_{yy}$ and $g_{zz} = 0$). In particular, we focus on the influence of electron correlation, basis set, equilibrium geometry, and zero-point vibrational contribution on these magnetic properties.

### 4.2.1 | Electron correlation

The obtained values for the isotropic magnetizability and the corresponding rotational $g$ tensors are listed in Table 4 for ScH and Table 5 for YH. Graphically, the change of $\xi$ with the used correlation method is shown in Figure 2 (we are not showing the analogous plots for the rotational $g$ tensor, being its behavior very similar, as expected from the corresponding theoretical relation in Equation (17)). In all cases, consideration of electron correlation changes the values of the isotropic magnetizability by a fairly large amount.

All calculations, even those at the HF level, predict both molecules to be paramagnetic. However, as expected from the Reference 4, the paramagnetic behavior of ScH is more pronounced (by a factor of roughly 3) than the one of YH. Again, the trends in the calculations for ScH using the cc-pV5Z and cc-pwCV5Z basis sets are different. First of all, the use of the core-polarized basis set leads to much larger absolute values in the magnetizability, when electron-correlation is introduced (at the HF level, the two basis sets lead to more or less the same result). In particular, when considering the molecule aligned to the $z$ axis, the cc-pV5Z calculation shows $\xi_{xx}=\xi_{yy}$ entries smaller than in HF, while using cc-pwCV5Z there are larger. Second, while electron-correlation treatments increase the absolute values in the cc-pV5Z computations, the opposite is true when using the cc-pwCV5Z basis set. Here, electron correlation slightly reduces the absolute value of the magnetizability. CCSD and CCSD(T) calculations yield slightly lower absolute values for the magnetizability compared to HF. The different results obtained with the cc-pVXZ and cc-pwCVXZ sets can be traced back to the fc approximation used in the cc-pVXZ calculations, indicating that the inclusion of core-valence correlation effects is quite important for the reliable prediction of the magnetic properties of ScH. For YH, the calculations with the uncontracted ANO-RCC basis set show the same trend as the cc-pwCV5Z calculations for ScH.

### 4.2.2 | Basis-set dependence

The influence of the used basis set on the isotropic magnetizability has been explored for ScH, using the cc-pVXZ and cc-pwCVXZ sets with X=T, Q, and 5. The data are shown in Table 6 and visualized in Figure 3. Going from the smaller to the larger basis sets, the isotropic magnetizability increases, the effect is more pronounced for the cc-pwCVXZ than for the cc-pVXZ set. Accordingly, the basis-set convergence seems to be faster for the cc-pVXZ sets, but due to the fc approximation in the cc-pVXZ calculations, the limiting values are different for the valence and core-valence sets with the latter leading to larger absolute values for the isotropic magnetizability. Core-valence

**TABLE 3** Equilibrium geometries $R$ (in Ångström) and energies $E$ (in Hartree) from CCSD(T) calculations of ScH with varying basis sets, that is, those of the cc-pVXZ and cc-pwCVXZ families with $X = T, Q$, and 5.

| Basis | $E$ | $R$ |
|---|---|---|
| cc-pVTZ | −760.3634 | 1.7922 |
| cc-pVQZ | −760.3655 | 1.7924 |
| cc-pV5Z | −760.3663 | 1.7925 |
| cc-pwCVTZ | −760.8600 | 1.7643 |
| cc-pwCVQZ | −760.9094 | 1.7602 |
| cc-pwCV5Z | −760.9550 | 1.7574 |

**TABLE 5** Isotropic magnetizability $\xi$ (in atomic units) and rotational $g$ tensor values for YH.

| | $\xi$ | $g$ |
|---|---|---|
| HF | 4.5520 | −8.0429 |
| CCSD | 5.9018 | −8.3790 |
| CCSD(T) | 6.4492 | −8.5919 |

*Note*: Calculations were performed with the uncontracted ANO-RCC basis set; the molecular geometry has been fixed to the CCSD(T)/uncontracted ANO-RCC bond length.

| $\xi$ | cc-pV5Z | cc-pwCV5Z | $g$ | cc-pV5Z | cc-pwCV5Z |
|---|---|---|---|---|---|
| HF | 15.5233 | 15.4968 | HF | −13.7431 | −13.7282 |
| CCSD | 12.3364 | 18.4768 | CCSD | −11.8482 | −15.1090 |
| CCSD(T) | 13.6091 | 19.1976 | CCSD(T) | −12.5543 | −15.4885 |

*Note*: Calculations were performed with the cc-pV5Z and cc-pwCV5Z basis sets. The molecular geometry has been fixed to the CCSD(T)/cc-pwCV5Z bond length.

**TABLE 4** Isotropic magnetizability $\xi$ (in atomic units) and rotational $g$ tensor values for ScH.

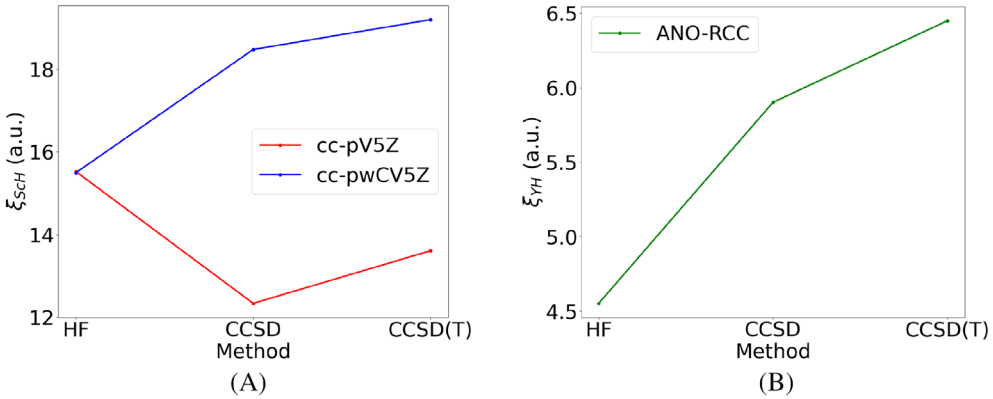


**FIGURE 2** Isotropic magnetizabilities (in atomic units) of ScH (left) and YH (right) calculated at CCSD, and CCSD(T) levels of theory. The red line corresponds to ScH with cc-pV5Z basis set, the blue one to ScH with cc-pwCV5Z and the green one to YH with ANO-RCC basis set.

**TABLE 6** Isotropic magnetizability $\xi$ (in atomic units) and rotational $g$ tensor values for ScH.

| $\xi$ | CCSD(T) | $g$ | CCSD(T) |
|---|---|---|---|
| cc-pVTZ | 13.2045 | cc-pVTZ | −12.3398 |
| cc-pVQZ | 13.5004 | cc-pVQZ | −12.4973 |
| cc-pV5Z | 13.6091 | cc-pV5Z | −12.5543 |
| cc-pwCVTZ | 17.4022 | cc-pwCVTZ | −14.5161 |
| cc-pwCVQZ | 18.7355 | cc-pwCVQZ | −15.2394 |
| cc-pwCV5Z | 19.1976 | cc-pwCV5Z | −15.4885 |

*Note*: Calculations were performed at CCSD(T) level of theory, varying the basis set in the frame of the cc-pVXZ and cc-pwCVXZ families. The molecular geometry has been fixed to the CCSD(T)/cc-pwCV5Z bond length.

correlation effects clearly need to be considered to obtain accurate values for the magnetizability of ScH.

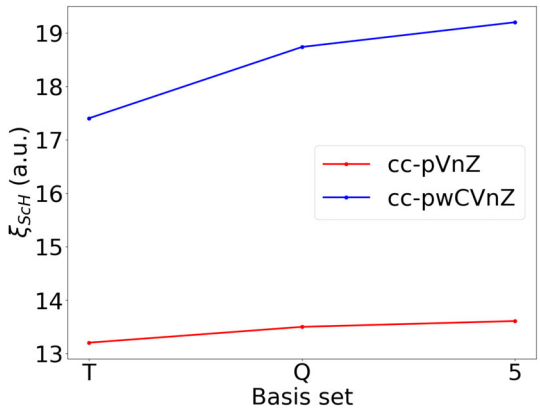


**FIGURE 3** Isotropic magnetizabilities of ScH calculated at CCSD(T) level of theory, with varying basis set. The red line corresponds to the cc-pVXZ family, the green one to the cc-pwCVXZ one.

### 4.2.3 | Equilibrium geometry

In the following section, the influence of the used equilibrium geometry on the computed magnetic properties is investigated. For both molecules, calculations using different geometries were performed at the CCSD(T) level of theory. For ScH, the results are listed in Table 7, for geometries optimized with the cc-pV5Z and the cc-pwCV5Z basis sets. As expected, there is no significant difference between the results obtained with the CCSD(T) and CCSDT geometries, as the perturbative treatment of triple excitations in CCSD(T) is known to be an excellent approximation to the full treatment of triple excitations at the CCSDT level. Finally, the red (cc-pV5Z) and blue line (cc-pwCV5Z) are fairly parallel, showing higher absolute values for the cc-pWCV5Z calculations.

The adoption of the cc-pwCV5Z basis set in the geometry optimization reverses the trend when going from CCSD to CCSD(T); again, the change when going from the CCSD to the CCSD(T) geometry is very small.

Calculations for YH (see Table 8) show a small increase when accounting for perturbative triple excitations in the geometry optimization.

As a common consideration, the most consistent choice for a high-level CC calculation of magnetic properties is to use at least CCSD(T) for the preliminary geometry optimization, given the fact that it has a non-negligible influence on the value of the isotropic magnetizability.

Note that the biggest effect on the magnitude of the magnetizability is still given by the chosen correlation method; the optimized geometry in particular has an impact smaller by more than one order of magnitude.

### 4.2.4 | Zero-point vibrational corrections

The computed equilibrium values for the magnetic properties of ScH and YH are compared to their vibrationally averaged counterparts in Tables 9 and 10. The differences due to the consideration of vibrational effects are small for both for the isotropic magnetizability and the rotational $g$ tensor. For the magnetizabilities, $\xi$(vib) are slightly larger than the zero-point values $\xi$. There is no unique trend for the rotational $g$ tensor, but in all cases the differences are very small (the largest is seen for cc-pVQZ/CCSD(T) in ScH with about 0.0099%).

**TABLE 7** Isotropic magnetizability $\xi$ (in atomic units) and rotational $g$ tensor values for ScH.

| $\xi$ (CCSD(T)) | cc-pV5Z | cc-pwCV5Z |
|---|---|---|
| opt. cc-pV5Z | | |
| *R*[CCSD] | 13.4514 | 19.0405 |
| *R*[CCSD(T)] | 14.4327 | 19.9855 |
| *R*[CCSDT] | 14.4367 | 19.9892 |
| opt. cc-pwCV5Z | | |
| *R*[CCSD] | 14.3906 | 19.9465 |
| *R*[CCSD(T)] | 13.6091 | 19.1976 |
| ***g* (CCSD(T))** | **cc-pV5Z** | **cc-pwCV5Z** |
| opt. cc-pV5Z | | |
| *R*[CCSD] | −12.5205 | −15.3288 |
| *R*[CCSD(T)] | −12.5195 | −15.3207 |
| *R*[CCSDT] | −12.5194 | −15.3199 |
| opt. cc-pwCV5Z | | |
| *R*[CCSD] | −12.5649 | −15.5232 |
| *R*[CCSD(T)] | −12.5543 | −15.4885 |

*Note*: Different equilibrium geometries, indicated as R[method, basis], were chosen to calculate the magnetic properties at CCSD(T)/cc-pV5Z and CCSD(T)/cc-pwCV5Z level.

**TABLE 8** Isotropic magnetizability $\xi$ (in atomic units) and rotational $g$ tensor values for YH.

| Geometry | $\xi$ | $g$ |
|---|---|---|
| *R*[CCSD] | 6.4450 | −8.5982 |
| *R*[CCSD(T)] | 6.4492 | −8.5919 |

*Note*: Different equilibrium geometries, indicated as R[method, basis], were chosen to calculate the magnetic properties at CCSD(T)/uncontracted ANO-RCC level.

**TABLE 9** Results for magnetic properties $\xi$ (in atomic units), $g$ and the corresponding vibrationally averaged values $\xi$,$g$(vib) for ScH.

| cc-pVQZ | $\xi$ | $\xi$(vib) | $\Delta\xi$ | $\Delta\xi$ [%] |
|---|---|---|---|---|
| CCSD | 12.9199 | 13.5535 | 0.6336 | 4.9037 |
| CCSD(T) | 14.3183 | 15.0864 | 0.7680 | 5.3640 |
| cc-pwCVQZ | | | | |
| CCSD | 17.6790 | 18.1087 | 0.4297 | 2.4306 |
| CCSD(T) | 18.7958 | 19.2751 | 0.4793 | 2.5500 |
| **cc-pVQZ** | $g$ | $g$(vib) | $\Delta g$ | $\Delta g$ [%] |
| CCSD | −11.7377 | −11.8234 | −0.0856 | −0.0073 |
| CCSD(T) | −12.4631 | −12.5864 | −0.1233 | −0.0099 |
| cc-pwCVQZ | | | | |
| CCSD | −14.7894 | −14.7489 | 0.0404 | 0.0027 |
| CCSD(T) | −15.2264 | −15.1833 | 0.0431 | 0.0028 |

*Note*: We list also the differences between the two quantities: $\Delta\xi = \xi(\text{vib}) - \xi$ while $\Delta\xi$ [%]$= \Delta\xi/\xi$. Calculations were performed with the cc-pVQZ and cc-pwCVQZ basis sets and CCSD and CCSD(T) levels of theory.

**TABLE 10** Results for magnetic properties $\xi$ (in atomic units), $g$ and the corresponding vibrationally averaged values $\xi$,$g$(vib) for YH.

| Method | $\xi$ | $\xi$(vib) | $\Delta\xi$ | $\Delta\xi$ [%] |
|---|---|---|---|---|
| CCSD | 5.8979 | 5.9986 | 0.1007 | 0.0171 |
| CCSD(T) | 6.4492 | 6.5669 | 0.1177 | 0.0182 |
| **Method** | $g$ | $g$(vib) | $\Delta g$ | $\Delta g$ [%] |
| CCSD | −8.3853 | −8.3359 | 0.0494 | 0.0059 |
| CCSD(T) | −8.5919 | −8.5439 | 0.0480 | 0.0056 |

*Note*: We list also differences between the two quantities: $\Delta x = x(\text{vib}) - x$ while $\Delta x$ [%]$= \Delta x/x$ for $x = \xi, g$. All calculations were performed with the uncontracted ANO-RCC basis and CCSD and CCSD(T) levels of theory.

In general, the zero-point vibrational corrections in $\xi$ are larger by two orders of magnitude for ScH, when comparing to YH. Also, the cc-pVQZ basis set mostly yields larger differences than the cc-pwCVQZ set. For all calculations, CCSD and CCSD(T) show the same behavior, slightly increasing the magnitude of the vibrational corrections when going from CCSD to CCSD(T).

The main concern was to find out whether a consideration of zero-point vibrational effects influences the magnetizability to such an extent that it jeopardizes the paramagnetic behavior of ScH and YH. However, both hydrides are after consideration of these effects still found to have a rather large positive value of $\xi$.

From these calculations it is clear that the inclusion of vibrational effects has a minimal influence on the calculated magnetizabilities.

## 5 | CONCLUSIONS

In the present work, the magnetic properties of the two transition-metal hydrides ScH and YH have been analyzed with respect to a possible paramagnetic behavior. All calculations and in particular those at the CC level using large basis sets predict that these two hydrides indeed show closed-shell paramagnetism similar to the one already predicted for BH and $CH^+$. Our best values including zero-point vibrational corrections for the isotropic magnetizabilities of ScH and YH are $\xi_{ScH}$=19.2751 a.u. and $\xi_{YH}$=6.5669 a.u. The reliability of our prediction has been checked in several ways, that is, by investigating the importance of electron correlation at CCSD, CCSD(T), and even CCSDT level, by analyzing the basis-set convergence, the influence of the used geometry in the computations and by accounting for zero-point vibrational effects. Among these, the consideration of core-valence correlation has the largest effect, while geometry, electron-correlation method, and basis-set choice have a much less pronounced influence and can be considered less critical. Zero-point vibrational effects are considered in order to provide values that are of experimental relevance. We also report predictions for the rotational $g$ tensor of ScH and YH, namely $g_{ScH} = -15.1833$ and $g_{YH} = -8.5439$. The measurement of the corresponding rotational spectra in an external magnetic field might be the easiest way to prove the here predicted closed-shell paramagnetism of ScH and YH.

The only shortcoming of our computations is the neglect of relativistic effects, but we do not expect that their consideration will change our results dramatically. Relativistic effects are most likely more pronounced for YH than ScH, as the latter hydride involves a light transition metal. Future quantum-chemical investigations might aim at finding other candidates for closed-shell paramagnetism. Obvious targets are here, for example, systems such as $TiH^+$ or $ZrH^+$, but initial computations indicate that these systems might exhibit a rather strong multireference character and that complete active-space self-consistent field (CASSCF) treatments are required to obtain a correct description.

## ACKNOWLEDGMENTS

This article is dedicated to Professor Elfi Kraka on the occasion of her 70th birthday in 2022. One of the authors (J.G.) thanks Elfi for more than 40 years of friendship, the hospitality during several visits to Göteborg and Dallas, and collaboration in various scientific projects. This project was started during a stay of S.S. and J.G. at the Centre of Advanced Studies at the Norwegian Academy of Science and Letters in Oslo within the project "Molecules in Extreme Environments". Open Access funding enabled and organized by Projekt DEAL.

## DATA AVAILABILITY STATEMENT

The data that support the findings of this study are available from the corresponding author upon reasonable request.

## ORCID

*Jürgen Gauss* https://orcid.org/0000-0002-6432-9345

## REFERENCES

[1] J. H. Van Vleck, *Phys. Rev.* **1927**, *29*, 727.
[2] J. H. Van Vleck, *Phys. Rev.* **1928**, *31*, 587.
[3] J. H. Van Vleck, *The Theory of Electric and Magnetic Susceptibilities*, Oxford University Press, Oxford **1932**.
[4] S. P. A. Sauer, T. Enevoldsen, J. Oddershede, *J. Chem. Phys.* **1993**, *98*, 9748.
[5] R. A. Hegstrom, W. N. Lipscomb, *J. Chem. Phys.* **1966**, *45*, 2378.
[6] C. T. Corcoran, J. O. Hirschfelder, *J. Chem. Phys.* **1980**, *72*, 1524.
[7] P. Fowler, E. Steiner, *J. Chem. Phys.* **1992**, *97*, 4215.
[8] T. Rebane, *Zh. Eksp. Teor. Fiz.* **1960**, *38*, 963.
[9] R. A. Hegstrom, W. N. Lipscomb, *Rev. Mod. Phys.* **1968**, *40*, 354.
[10] S. P. A. Sauer, J. F. Ogilvie, *J. Phys. Chem.* **1994**, *98*, 8617.
[11] J. Guy, J. Tillieu, J. Baudet, *C. R. Hebd. Seances Acad. Sci.* **1958**, *246*, 574.
[12] J. Tillieu, *Ann. Phys.* **1957**, *13*, 631.
[13] P. G. Lykos, *J. Am. Chem. Soc.* **1966**, *88*, 4309.
[14] F. London, *J. Phys. Radium* **1937**, *8*, 397.
[15] H. F. Hameka, *Mol. Phys.* **1958**, *1*, 203.
[16] R. Ditchfield, *J. Chem. Phys.* **1972**, *56*, 5688.
[17] K. Wolinski, J. F. Hinton, P. Pulay, *J. Am. Chem. Soc.* **1990**, *112*, 8251.
[18] J. Gauss, *Chem. Phys. Lett.* **1992**, *191*, 614.
[19] K. Ruud, T. Helgaker, K. L. Bak, P. Jørgensen, H. J. A. Jensen, *J. Chem. Phys.* **1993**, *99*, 3847.
[20] C. Møller, M. S. Plesset, *Phys. Rev.* **1934**, *46*, 618.
[21] G. D. Purvis III, R. J. Bartlett, *J. Chem. Phys.* **1982**, *76*, 1910.
[22] K. Raghavachari, G. W. Trucks, J. A. Pople, M. Head-Gordon, *Chem. Phys. Lett.* **1989**, *157*, 479.
[23] J. Noga, R. J. Bartlett, *J. Chem. Phys.* **1987**, *86*, 7041.
[24] G. E. Scuseria, H. F. Schaefer III, *Chem. Phys. Lett.* **1988**, *152*, 382.
[25] J. Gauss, J. F. Stanton, *Chem. Phys. Lett.* **1997**, *276*, 70.
[26] K. Ruud, P.-O. Åstrand, P. R. Taylor, *J. Chem. Phys.* **2000**, *112*, 2668.
[27] A. A. Auer, J. Gauss, J. F. Stanton, *J. Chem. Phys* **2003**, *118*, 10407.
[28] I. M. Mills, in Molecular Spectroscopy: Modern Research; *Rao, K. N* (Ed: C. W. Mathews), Academic Press, New York **1972**, p. 115.
[29] W. Schneider, W. Thiel, *Chem. Phys. Lett.* **1989**, *157*, 367.
[30] J. F. Stanton, C. L. Lopreore, J. Gauss, *J. Chem. Phys.* **1998**, *108*, 7190.
[31] W. H. Flygare, *Chem. Rev.* **1974**, *74*, 653.
[32] J. Gauss, K. Ruud, T. Helgaker, *J. Chem. Phys.* **1996**, *105*, 2804.
[33] T. H. Dunning Jr., *J. Chem. Phys.* **1989**, *90*, 1007.
[34] N. B. Balabanov, K. A. Peterson, *J. Chem. Phys.* **2005**, *123*, 064107.
[35] P.-O. Widmark, P.-A. Malmqvist, B. O. Roos, *Theor. Chem. Acta* **1990**, *77*, 291.
[36] B. O. Roos, R. Lindh, P.-Å. Malmqvist, V. Veryazov, P.-O. Widmark, *J. Phys. Chem. A* **2005**, *109*, 6575.
[37] J. Gauss, J. F. Stanton, R. J. Bartlett, *J. Chem. Phys.* **1991**, *95*, 2623.
[38] J. Gauss, J. F. Stanton, *J. Chem. Phys.* **2002**, *116*, 1773.
[39] M. Kállay, J. Gauss, P. G. Szalay, *J. Chem. Phys.* **2003**, *119*, 2991.
[40] T. Nottoli, J. Gauss, F. Lipparini, *Mol. Phys.* **2021**, *119*, e1974590.
[41] T. Yoshizawa, M. Hada, *J. Comput. Chem.* **2009**, *30*, 2550.
[42] M. Iliaš, H. J. A. Jensen, R. Bast, T. Saue, *Mol. Phys.* **2013**, *111*, 1373.
[43] T. Enevoldsen, T. Rasmussen, S. P. A. Sauer, *J. Chem. Phys.* **2001**, *114*, 84.
[44] J. F. Stanton, J. Gauss, L. Cheng, M. E. Harding, D. A. Matthews, P. G. Szalay, CFOUR, Coupled-Cluster Techniques for Computational Chemistry, a Quantum-Chemical Program Package. With Contributions From A. Asthana, A. A. Auer, R. J. Bartlett, U. Benedikt, C. Berger, D. E. Bernholdt, S. Blaschke, Y. J. Bomble, S. Burger, O. Christiansen, D. Datta, F. Engel, R. Faber, J. Greiner, M. Heckert, O. Heun, M. Hilgenberg, C. Huber, T.-C. Jagau, D. Jonsson, J. Jusélius, T. Kirsch, M.-P. Kitsaras, K. Klein, G. M. Kopper, W. J. Lauderdale, F. Lipparini, J. Liu, T. Metzroth, L. A. Mück, D. P. O'Neill, T. Nottoli, J. Oswald, D. R. Price, E. Prochnow, C. Puzzarini, K. Ruud, F. Schiffmann, W. Schwalbach, C. Simmons, S. Stopkowicz, A. Tajti, T. Uhlirova, J. Vázquez, F. Wang, J. D. Watts, P. Yergün, C. Zhang, X. Zheng, and the Integral Packages MOLECULE (J. Almlöf and P. R. Taylor), PROPS (P. R. Taylor), ABACUS (T. Helgaker, H. J. Aa. Jensen, P. Jørgensen, and J. Olsen), and ECP Routines by A. V. Mitin and C. van Wüllen. http://www.cfour.de
[45] D. A. Matthews, L. Cheng, M. E. Harding, F. Lipparini, S. Stopkowicz, T.-C. Jagau, P. G. Szalay, J. Gauss, J. F. Stanton, *J. Chem. Phys.* **2020**, *152*, 214108.
[46] S. Coriani, D. Marchesan, J. Gauss, C. Hättig, T. Helgaker, P. Jørgensen, *J. Chem. Phys.* **2005**, *123*, 184107.
[47] R. S. Ram, P. F. Bernath, *J. Chem. Phys* **1996**, *105*, 2668.
[48] J. Anglada, P. J. Bruna, S. D. Peyerimhoff, *Mol. Phys.* **1989**, *66*, 541.
[49] M. Hubert, J. Olsen, J. Loras, T. Fleig, *J. Chem. Phys.* **2013**, *139*, 194106.
[50] L. Lodi, S. N. Yurchenko, J. Tennyson, *Mol. Phys.* **2015**, *113*, 1998.
[51] R. S. Ram, P. F. Bernath, *J. Chem. Phys.* **1994**, *101*, 9283.
[52] K. Balasubramanian, J. Z. Wang, *J. Mol. Spectrosc.* **1989**, *133*, 82.
[53] T. Saue, *Chem. Phys. Chem.* **2011**, *12*, 3077.

**How to cite this article:** L. Grazioli, L. T. Schleicher, S. Stopkowicz, J. Gauss, *J. Comput. Chem.* **2024**, *45*(15), 1215. https://doi.org/10.1002/jcc.27305